흡배기구 손실예측 및 이를 고려한 항공기 가스터빈의 장착 성능모사 연구

공창덕* · George .Omollo. Owino**

Study on Installed Performance Simulation of Aircraft Gas-Turbine Engine Considering Inlet and Exhaust Losses

Changduk Kong* · George .Omollo. Owino**

ABSTRACT

Experimental study has been a general way to evaluate inlet and exhaust duct performances, but this is not only costly but also time consuming. Computational simulation is hence replacing experimental study and consequently time and cost saving. This paper therefore aims to investigate typical component performance of the intake and exhaust ducts using 3D representation. In this study a specific inlet and exhaust was modeled and analyzed to estimate its losses and flow field using computational fluid dynamic program with flow visualization capabilities. A process that requires geometry data to be modeled. That allowed for possibility of design trade off in designing phase. Installed performance of a specific turbo shaft engine was finally evaluated with the estimated inlet, exhaust and other accessories losses.

초 록

실험적인 연구가 흡입구와 배기구 성능을 평가하는 일반적인 방법이나 이는 고가이며 많은 시간이 소요된다. 따라서 소요 시간과 계산을 절약하는 방법으로 전산 유체 역학적 수치 모사가 실험적 연구로 대체할 수 있다. 그러므로 본 연구는 3차원 형상 모델을 이용하여 흡입구와 배기구의 구성품 성능을 연구하는 것을 목표로 하였다. 본 연구에서 특정한 흡입구 및 배기구를 유동가시화 기능을 갖는 전산 유체 역학적 프로그램을 이용하여 손실 및 유동장을 예측하기 위해 모델링 및 해석이 수행되었다. 모델링된 기하학적 자료를 필요로 하는 과정이 설계과정에서 설계 개선 가능성을 위해 요구되었다. 또한 특정 터보축 엔진의 장착 성능이 예측된 흡입구, 배기구 및 기타 보기 손실을 가지고 평가되었다.

Key Words: Installed performance(엔진 장착 성능), Inlet and Exhaust duct losses(흡배기구 손실), Turbo Shaft Engine(터보축 엔진), CFD simulation(전산유체 시뮬레이션).

† 2006년 11월 13일 접수 ~ 2006년 12월 13일 심사완료
* 종신회원, 조선대학교 항공우주공학과
** 학생회원, 조선대학교 항공우주공학과 대학원
연락저자, E-mail: cdgong@chosun.ac.kr

1. Introduction

Gas turbine engines are designed to provide thrust at all possible operating conditions within

the flight envelop that they are designed. It is expected therefore that the engine inlet ducts deliver air Mass flow rate at the correct speed, angle and flow pattern that ensures optimum operation with minimal losses within the ducts.

A way of predicting the performance losses plays a major role in ensuring good design of engine ducts, nacelle and plenum chamber at low cost and reliable practical flow regimes that may be used in the aircraft propulsion system.

Three dimension numerical simulation of the whole engine is the leading edge research method the scale of such computation, however limits its application on design procedure of aero-engines.

2. Inlet and Exhaust Duct Loss Estimation

2.1 Operating conditions

For this study a divergent inlet duct that connects to the engine side intake using a plenum chamber with a Mass flow rate of 5.1884lb/s at a cruise velocity of Mach 0.4 was analyzed

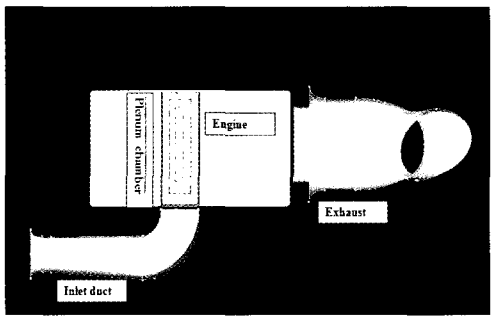

Fig. 1 schematic diagram of Intake, engine and exhaust

If the engine geometry and specification are given, sizing of the inlet duct is done using the flow function

$$\frac{\dot{M}\sqrt{T_t}}{AP_t} = M_n K \qquad (1)$$

where

$$k = \sqrt{\left\{\frac{\gamma}{R\left[1+\left(\frac{\gamma-1}{\gamma}\right)M_n\right]^{\frac{\gamma+1}{\gamma-1}}}\right.} \qquad (2)$$

Tt A Mn and P_t are the temperature, area, Mach number and pressure at the throat respectively.

Table 1. PW206C Engine operation range

Parameter	Range
Operational flight altitude (ft)	10000
Turbine inlet temperature (R)	2258
Flight mach number	0~0.4

From ambient pressure we can obtain the value of inlet pressure assuming isentropic compression. starting from ambient pressure then

$$P_0 = P_a * e^{\psi(T_0)-\psi(T_{amb})} \qquad (3)$$

where (entropy function)

$$\Psi(T) = \frac{1}{R}\int_{T_{ref}}^{T}\frac{c_p(T)}{T}dT \qquad (4)$$

2.2 Mass flow rate

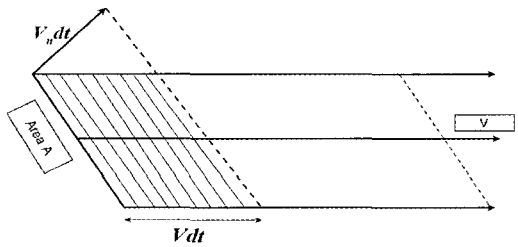

Fig. 2 Mass flow through a flow field

Air mass flow rate at any station within the intake duct remains constant and may be calculated considering Fig. 2 If an air mass (M) sweeps over area (A shaded) at time interval (dt). then Mass flow rate can be expressed as:

$$\dot{M} = \frac{\rho(V_n dt)A}{dt} \qquad (5)$$

Calculations are done assuming that density remains constant at 0.909kg/ m^3 in accordance to dimensions and sizes generated by the flow function.

Table 2. Calculated mass f low rate

	Throat	Elbow	Exit
Area (mm^2)	20.126	20.176	72.760
Velocity (m/s)	0.28	0.218	0.078
Mass flow (lb/s)	5.1884	5.1884	5.1884

Once all these variables have been calculated at each location performance simulation is performed to obtain pressure, temperature and mass flow rate at the compressor face.

2.3 Procedure to derive intake boundary parameters

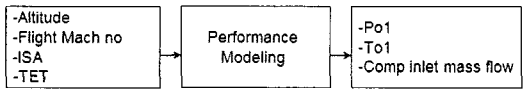

Fig. 3 procedure to derive inlet boundary conditions

Figure 3 represents the procedure used to obtain intake boundary conditions.

Performance modeling starts using ISA calculations for the used specified engine and range given on Table 1, steady state simulation to obtain, P_{01}, T_{01} and compressor inlet air flow rate is performed data which are used as input boundary condition for the duct exit.

Table 3. Input boundary conditions

Altitude ft	Temp (K)	Pressure (Pa)	Density (Kg/m^3)	Sonic.vel. (m/s)	Viscosity (M^2/s)
10000 Static	268.6	70121	0.909	328.5	1.86*10^-5
10000 Mach0.43	270.2	103930	-	-	-

It is important that inlet boundary conditions are defined with maximum accuracy .The intake duct used in this study is so design that there is an area difference between the lip face and the throat as can be seen in figure 4 and table 2 . Table 1 gives us the free stream Mach number to be between 0 and 0.4.

We should note the difference in Mach number from 0.4 free stream flow to 0.43 at the throat acceleration due to pressure reduction

2.4. Subsonic intake modeling considerations

The design process for the intake and nacelle geometry compromises the following steps

-Sizing of the intake
-Internal intake design parameters
-Design of the internal lip contour
-Design of the diffuser section

Because the air intake face limits the mass flow that can enter the engine, implies therefore that the throat having the smallest area has to perform in a way as to meet the maximum flow demand of the engine.

It is important to size the intake according to the highest flow point to ensure no choking at any flight envelope [3]

Figure 4 shows a typical intake arrangement of the aircraft gas turbine.

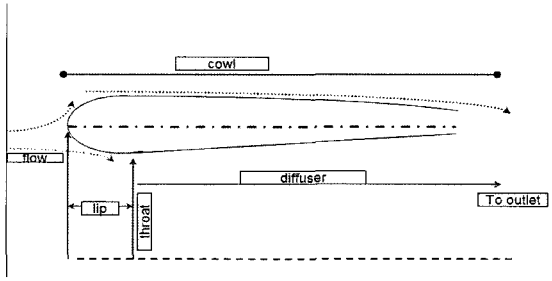

Fig. 4 Intake description

2.5 CFD modeling of duct

Once geometry is established then several issues have to be considered as follows;

-Shape and size of computational domain

-Grid structure and geometry

-Boundary conditions

-Solver setting

A 3-D axi- symmetric model with structured mesh was used for this study. Structured grid was selected as it allows the grid to be aligned with the flow direction within the domain and thus improves accuracy.

Figure 5 shows a structured meshed intake duct without the plenum chamber of about 61034 elements generated using CFD-GEOM tool.

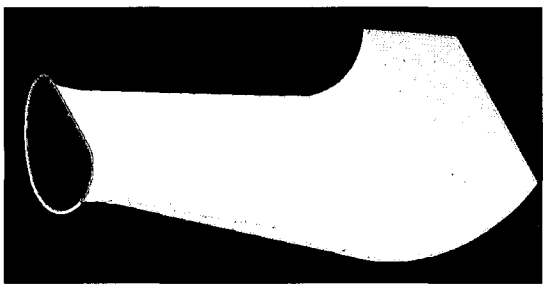

Fig .5 Structured grid of intake duct

Grid density used was of 20 to 30 nodes along the span wise length of the duct and 15 nodes for width. Reynolds Navier strokes (RANS) was used together with the wall functions.

Standard $k-\varepsilon$ model and Kato launder $k-\varepsilon$ model as aero duct require smooth interior ducts surface to minimize losses.[1]

The model was then exported to CFD-ACE solver where boundary conditions are defined. Pressure was selected to be the reference point as this study involves pressure loss.

2.6. Matching of performance and CFD simulation

The idea of combining CFD module and performance simulation requires an iteration procedure.

CFD analysis is performed with ideal boundary condition, predicted for the given air Mass flow rate. The simulated Mass flow rate reduction is observed due to pressure loss until engine is matched.

Component mass flow rate matching required several iteration performed at a cruise altitude of 10000ft and flight Mach Number 0.4 preselected condition to avoid duct choking.

2.7 Analysis results

According to the inlet duct CFD analysis results based on the given boundary conditions pressure loss was found to be about 2.3% for the intake duct model operating at a cruise condition of 10000ft Mach No 0.4 and mass flow rate 5.1884lb/s.

Table 4 CFD Analysis result

Parameter	inlet	outlet
Density Kg/m^3	0.957	0.9916
Mach No	0.435	0.31
Pressure (Pa)	103930	101239
Temperature (K)	268.0	270.29
Velocity U (m/s)	145	26.38

Based on this CFD results pressure loss within the duct can be calculated from the following equations. Percentage pressure loss can be expressed by

$$\frac{\Delta P_0}{P_{0a}} = 100(1-\eta_r)*\left(\frac{P_{0a}-P_a}{P_{0a}}\right) \quad (6)$$

where ram efficiency is defined as;

$$\eta_r = \frac{p_{01} - p_a}{p_{0a} - p_a} \quad (7)$$

and $$P_{0a} = P_a\left(1 + \frac{\gamma - 1}{2} M_a^2\right) \quad (8)$$

Table 5 shows the estimated pressure losses of the inlet using CFD analysis and equation 6 at several operating conditions.

Table 5. Estimated Pressure Losses of inlet at several conditions

(Mach No.)	0.1	0.2	0.3	0.4
Mass Flow (lb/s)	5.1884	5.1884	5.1884	5.1884
CFD Input.pres(Pa)	70119.68	71650.32	74173.8	77807.34
Output press (Pa)	68506.26	70417.93	73320.80	76990.36
pressure loss (%)	1.05	1.15	1.72	2.3

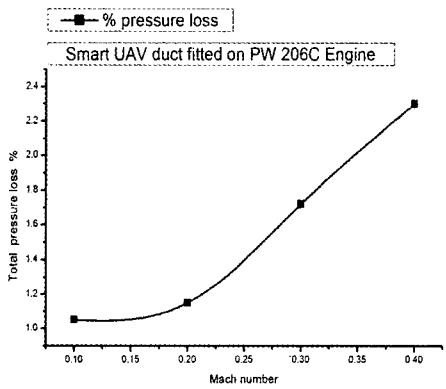

Fig. 6 Pressure loss with mach number variations

A constant increase in pressure loss with increasing Mach number was observed to a maximum pressure loss of 2.3% at mach 0.4

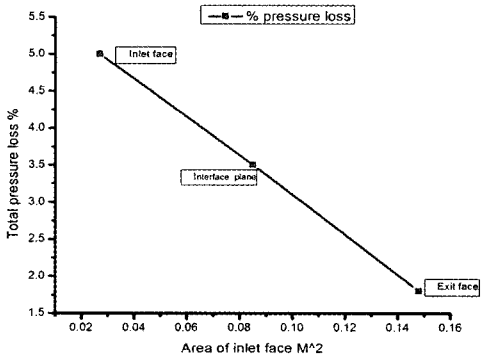

Fig. 7 Pressure loss with changing area along the duct length

Total pressure loss reduce with increase in area that may be associated with increase in volume at constant density and increase in airflow speed to maintain constant Mass flow rate.

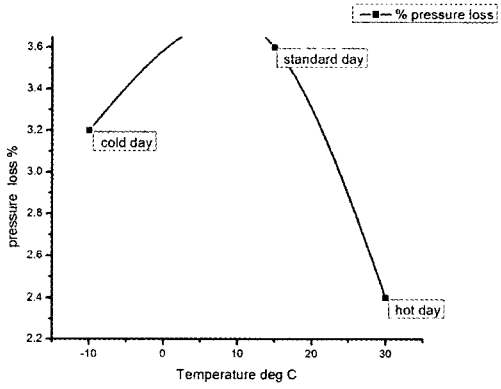

Fig. 8 Pressure loss with changes in inlet ambient temperature

Analysis done at different inlet temperature showed considerable low pressure loss on a hot day a phenomenon that is associated with reduced Mass flow rate from the normal 5.1884lb/s to 3.96lb/s for the same altitude and speed . Mass flow rate of 4.63lb/s for cold day

Figures 9, 10 and 11 show internal flow pattern, pressure distribution and pressure distortion, respectively.

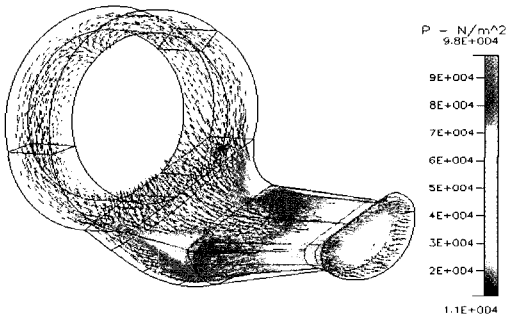

Fig 9. Intake duct air flow pattern

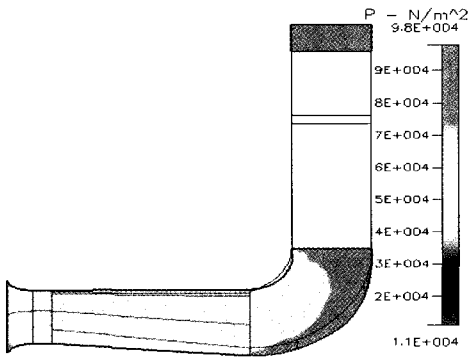

Fig 10. Pressure distribution as viewed from the Z plane cut

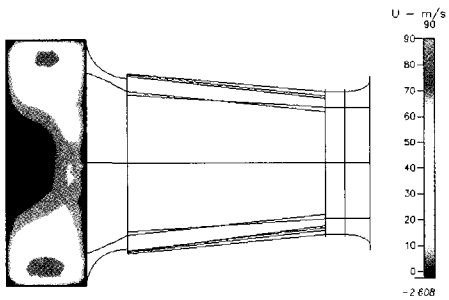

Fig. 11 Pressure distortion along interface plane between intake duct and plenum chamber

2.8 Exhaust Duct

The process of grid generation is more like that for the intake duct above except that unstructured grid was used with about 20000 elements. Two sets of inlet boundary conditions were used the main hot duct and cooling air duct

The core receives hot gasses at 887K projected at 160m/s and total inlet Mass flow rate (5.1884lb/s) remains constant since the engine and components match.

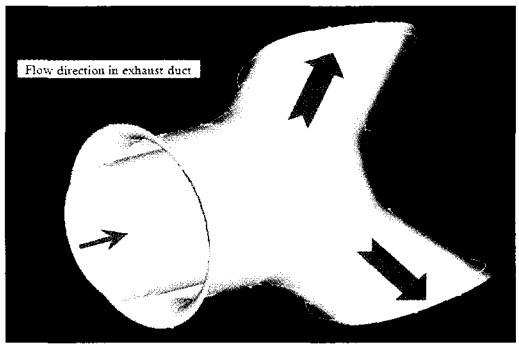

Fig. 12 Exhaust duct model

Table 6 below represents the CFD analysis results of the Exhaust duct and Table 7 shows the percentage pressure losses at several operating conditions. [5][6]

Table 6. CFD analysis results of the exhaust duct

Turbine exit flow	inlet	outlet
Temperature (K)	887	626.8
Mass flow rate (Lb/s)	5.1884	5.1884
Pressure (Pa)	183.800	157.6

Table 7. Estimated % Pressure losses of exhaust at several conditions

Conditions	Pressure loss
10000ft ISA Mach 0.1	1.499%
Hot day ISA+20 10000ft	1.32%
10000ft Mach 0.2 ISA	2.24%

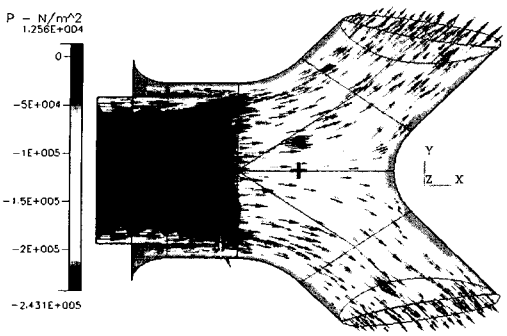

Fig. 13 flow contour of exhaust duct

3. Installed Performance of Turbo Shaft Engine

A commercial simulation program GASTURB 9 was used for this study .Several input values of RPM, Mach No were defined and the corresponding off design output value of Mass flow rate ,Fuel flow rate were obtained and compared to the corresponding condition as given by the EEPP (estimated engine performance program)[2]

Having analyzed the losses incurred at the intake (2.3%) and exhaust (1.499%) at Mach 0.4 they are included in the study of engine installed performance loss at ECS (environmental control systems) off and at Max

Analysis is done with variation of Gas generator RPM, Mach number and altitude respectively [4].

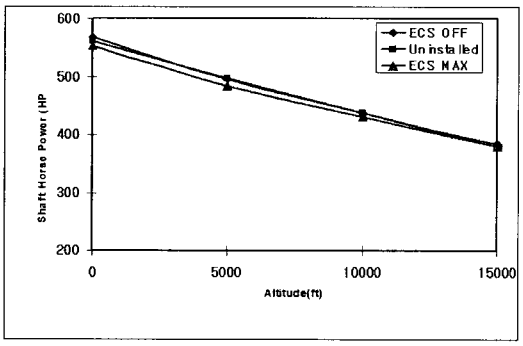

Fig. 14 Variations of Altitude

Shaft horse power reduces with increasing altitude with a slight loss in power at ECS Max due to power extraction and changes in air density that affects the Mass flow rate ,Mach 0.4 and gas generator speed of 100% was maintained.

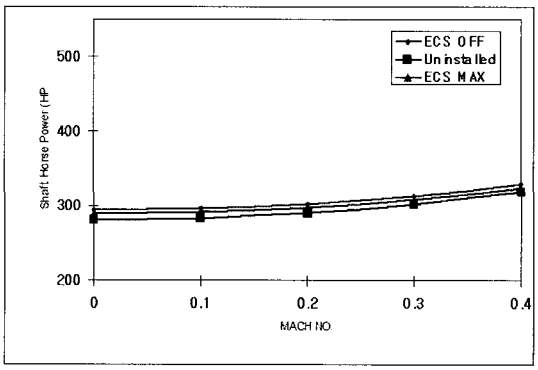

Fig. 15 Variations of Mach number

Variations of Mach numbers performed at 10000ft and Mach number 0.4 shows an increase in shaft horse power as a result is increased air supply to the duct face ECS Max is lower than ECS off due to mechanical losses gas generator speed of 60% was kept all through.

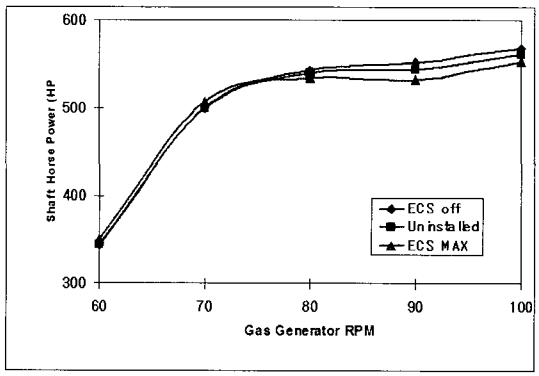

Fig. 16 Variations of Gas Generator Speed

Sea level static conditions at Mach number of 0.4 were used as gas generator speed was changed and corresponding values of shaft

horse power plotted against changes in RPM between 60~100%.

constant increase in power was observed until the rated power of 550 HP was reached.

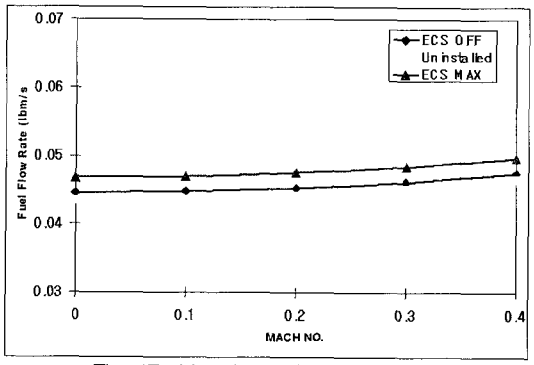

Fig. 17 Variations of Mach number

We observe slight increase in fuel flow rate with increasing Mach number that may be explained in terms of the extra power required to overcome the extra work done by the compressor 10000ft with 100% RPM was kept through this analysis.

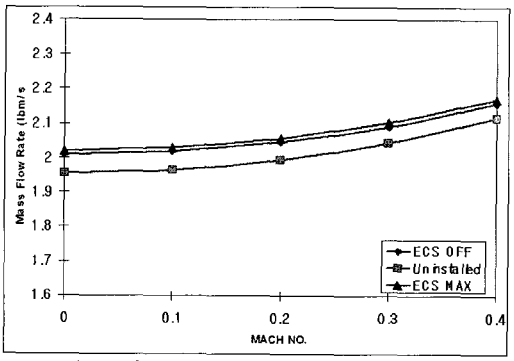

Fig. 18 Variations of Mach number

100% RPM at 10000ft observed similar trends as fuel flow rate Mach number increases the air Mass flow rate to the engine. that results in more power being produced

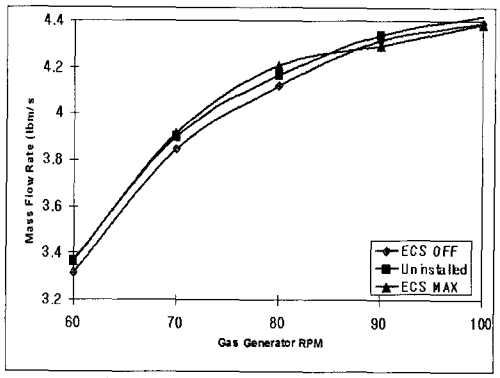

Fig. 19 Variations of Gas Generator Speed

The Mass flow rate at 10000ft with a speed of Mach 0.4 was plotted against changes of gas generator speed an increase of Mass flow rate what noticed. This works in accordance to the Mass flow rate formulae Equation 5.

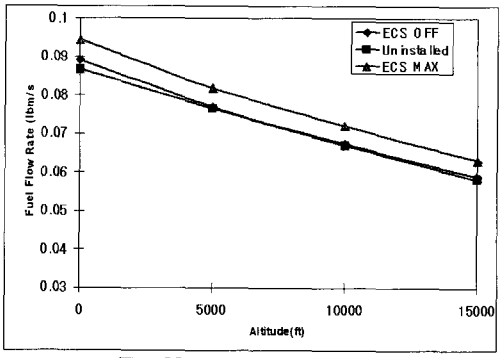

Fig. 20 Variations of Altitude

Proportional to the reduction in air density and Mass flow a corresponding reduction in fuel flow rate was noticed regardless of maintaining RPM at 100%

4. Conclusion

Due to lack of performance data fundamental design principles were applied to create a generic model. The results for each component appeared reasonable and CFD analysis of ducts was adapted easily to other ducts. The combination of CFD module for intake systems has shown reasonable results in absence of information about pressure losses for these components. Finally the installed performance of turbo shaft engine PW206C was investigated considering the calculated inlet losses estimated by CFD technique.

Acknowledgement

Thanks to Dr C. Lee of KARI for having provided initial inlet geometry and dimensions

Reference

1. Victoria Nichols, "intake modeling of a civil aero engine by CFD tool", Thesis, Cranfield University Press, 2005
2. Changduk Kong et al., "Component map generation of gas turbine engine using engine performance deck", ASME TURBO EXPO 2006 proceedings, 2006
3. J.Kurzke,"Effect of inlet flow distortion on performance of gas turbine", ASME TURBO EXPO 2006 proceedings, 2006
4. George et al., "Analysis of installed and un-installed performance of turbo shaft engine", 24th KSPE conference proceedings, 2006
5. Asim Maqsood, "Experimental and CFD study of exhaust ejectors with bent mixing tubes", ASME TURBO EXPO 2005 proceedings, 2005
6. Rao, G. V. R., "Exhaust Nozzle Contour for Maximum Thrust," Jet Propulsion, Vol. 28, No. 0, June, 1958, pp.377-382